

This is an Open Access document downloaded from ORCA, Cardiff University's institutional repository: <https://orca.cardiff.ac.uk/id/eprint/128180/>

This is the author's version of a work that was submitted to / accepted for publication.

Citation for final published version:

Wilson, Andrew S. S., Dinoi, Chiara, Hill, Michael S., Mahon, Mary F., Maron, Laurent and Richards, Emma 2020. Calcium hydride reduction of polycyclic aromatic hydrocarbons. *Angewandte Chemie International Edition* 59 (3) , pp. 1232-1237. 10.1002/anie.201913895

Publishers page: <http://dx.doi.org/10.1002/anie.201913895>

Please note:

Changes made as a result of publishing processes such as copy-editing, formatting and page numbers may not be reflected in this version. For the definitive version of this publication, please refer to the published source. You are advised to consult the publisher's version if you wish to cite this paper.

This version is being made available in accordance with publisher policies. See <http://orca.cf.ac.uk/policies.html> for usage policies. Copyright and moral rights for publications made available in ORCA are retained by the copyright holders.



Calcium Hydride Reduction of Polycyclic Aromatic Hydrocarbons

Andrew S. S. Wilson, Chiara Dinoi, Michael S. Hill,* Mary F. Mahon, Laurent Maron,* and Emma Richards

Abstract: A molecular calcium hydride effects the two electron reduction of polyaromatic hydrocarbons, including naphthalene ($E^0 = @3.1$ V).

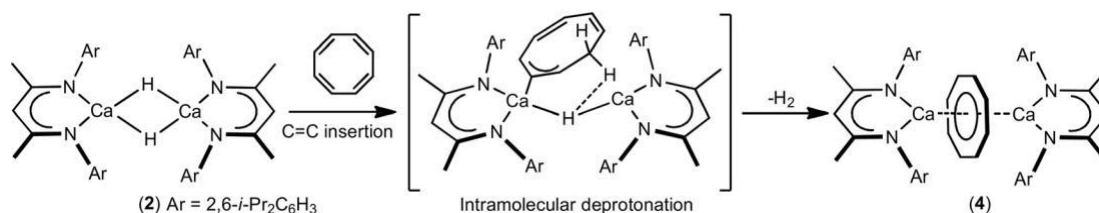
Hydride derivatives have provided a focal point for many recent advances in molecular alkaline earth (Ae = Mg, Ca, Sr and Ba) chemistry.^[1–3] Instigated by Harder and co-workers report of the calcium hydride, $[(\text{DippBDI})\text{Ca}(\text{THF})\text{H}]_2$ (**1**, $\text{DippBDI} = \text{HC}(\text{Me})\text{CN}-2,6\text{-}i\text{-Pr}_2\text{C}_6\text{H}_3$),^[4, 2] b-diketiminato derivatives have been especially prominent. The synthesis of a solvent-free analogue of **1** (**2**, see Scheme 1) highlights how a reduction in coordinative saturation at the calcium center can impact significantly on the observed chemistry.^[5] Compound **2** reacts with a wide range of unactivated terminal alkenes,^[4,6] providing *n*-alkyl derivatives, which are sufficiently nucleophilic to effect the heterolytic cleavage of H_2 or even the direct displacement of hydride from benzene.^[5,6] Subsequent use of a bulkier b-diketiminato ligand in the synthesis of $[(\text{DIPePBDI})\text{SrH}]_2$ (**3**; $\text{DIPePBDI} = \text{HC}(\text{Me})\text{CN}-2,6\text{-}(\text{Et}_2\text{CH})_2\text{C}_6\text{H}_3$) has shown that analogous reactivity may be achieved at strontium.^[3]

Computational analysis using density functional theory (DFT) indicated reactions of **2** with $\text{C}=\text{C}$ multiple bonds are highly polarized and proceed in a stepwise fashion with no necessary rupture of either the dinuclear hydride or the dinuclear hydrido-alkyl intermediates formed during the reactions. The dimeric structure of **2** is particularly significant

during its reaction with 1,3,5,7-cyclooctatetraene (COT) to yield the inverse sandwich dicalcium cyclooctatetraenyl $[\text{COT}]^{2@}$ derivative (**4**, Scheme 1).^[7] Although the two electron reduction of COT is typically achieved by its stepwise reaction with a suitable alkali metal,^[8] monitoring of the formation of **4** by EPR spectroscopy did not provide any evidence of single electron transfer or radicaloid intermediates. Rather, DFT analysis indicated that reduction proceeds via a pathway involving consecutive polarized $\text{Ca@H/C}=\text{C}$ insertion and intramolecular deprotonation, which is imposed by the retention of dicalcium species throughout the reaction.

This reactivity raises questions about the broader reductive potential of soluble molecular compounds such as **2** and **3**. Although the elemental Ae metals have been employed as electron sources ($E^0 = \text{Mg}, @2.36$; $\text{Ca}, @2.76$; $\text{Sr}, @2.90$; $\text{Ba}, @2.91$ V vs. SCE), more apposite examples of molecular group 2 reductants are provided by Jones and Stasch's dinuclear Mg^{I} species, such as $[(\text{DippBDI})\text{Mg}]_2$ (**5**) and $[(\text{MesBDI})\text{Mg}]_2$ (**6**) (Scheme 2), which have been posited as “quasi-universal” reducing agents.^[9] In contrast to the heterogeneous nature of any “dissolving metal” reduction, electron transfer from the hydrocarbon-soluble compounds **5** and **6** is facilitated by the relatively diffuse nature of the Mg-Mg -centered HOMO.

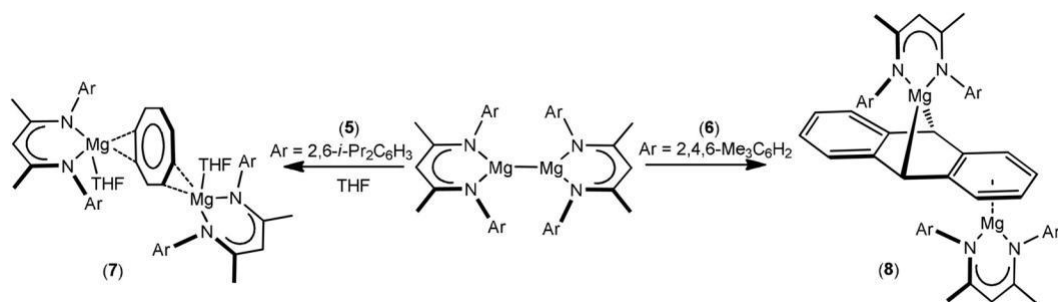
The stepwise reduction of polycyclic aromatic hydrocarbons (PAHs) such as naphthalene and anthracene has been studied since the mid-19th century.^[10] Unlike the 10p electron



Scheme 1. Sequential $\text{Ca@H/C}=\text{C}$ insertion and deprotonation pathway to compound **4**.

[*] Dr. A. S. S. Wilson, Prof. M. S. Hill, Dr. M. F. Mahon Department of Chemistry, University of Bath Bath, BA2 7AY (UK)
E-mail: msh27@bath.ac.uk
Dr. C. Dinoi, Prof. L. Maron
Universit de Toulouse et CNRS, INSA, UPS, UMR 5215, LPCNO 135 Avenue de Rangueil, 31077 Toulouse (France)
E-mail: laurent.maron@irsamc.ups-tlse.fr
Dr. E. Richards
School of Chemistry, Cardiff University
Park Place, Cardiff CF10 3AT (UK)

aromatization of COT to $[\text{COT}]^{2@}$, reduction involves disruption of the aromatic system and population of the relevant antibonding p^* LUMO. The total free energy of the system may be estimated from the PAH reduction potentials which increase, that is become less negative, with the number of constituent C_6 carbocycles. With regard to group 2, the reaction of anthracene ($E^0 = @1.98$ and $@2.44$ V vs. SCE) and magnesium is particularly well studied and, like the corresponding reactions with calcium, strontium and barium, can access the products of both single and two-electron reduction.^[11, 12] Reflecting the electrochemical data, however, only lithium among the elements of group 1 and 2 can effect twofold reduction of naphthalene ($E^0 = \text{ca. } @3.1$ V) to the $[\text{C}_{10}\text{H}_8]^{2@}$



Scheme 2. Two electron reduction of COT and anthracene by b-diketiminato Mg^I derivatives.

dianion,^[13] whereas liquid ammonia solutions of naphthalene and Ae metals yield only single electron reduction to produce the naphthalenide radical anion.^[12, 14]

Two electron reduction of COT ($E^0 = @1.83$ and $@1.99$ V vs. SCE) by 5, occurs readily to deliver the magnesium analogue of 4, compound 7 (Scheme 2). Treatment of anthracene by compound 6 also provides two-electron reduction and the formation of compound 8. While the electrochemical reduction potentials of 5 and 6 have never been determined, a very recent report of the six electron reduction of C₆₀ by 6 indicates a reducing capability which is at least in the order of $E^0 = @2.9$ V (vs. SCE).^[15] Consistent with this upper limit, however, such Mg^I species are indefinitely stable in benzene ($E^0 = ca. @3.4$ V) and no evidence of reactivity with naphthalene ($E^0 = ca. @3.1$ V) has been reported. Although any operant mechanisms are likely to be very different from the more direct electron transfer implicated in the formation of compounds 7 and 8 (*vide infra*), these observations highlight that the reactivity of 2 with a range of PAHs should provide a semi-quantitative means with which to assess its reducing potential.

Our study commenced with a consideration of the reactivity of 2 with the parent monocyclic arene, benzene. Reminiscent of the behaviour of the group 3 and 4f hydride derivatives, [Cp*₂MH]_n ($n = 1, M = Sc; n = 2, M = Y, La, Sm, Lu$),^[16] Harder has reported that moderate heating (60–80°C) of

a C₆D₆ solution of the molecular strontium hydride (3) provides complete H–D exchange with the deuterated solvent to provide [(^DiP^ePBDI)SrD]₂ and C₆D₅H within 12 hours.^[3] Analogous thermal treatment of a C₆D₆ solution of compound 2 resulted, primarily, in Schlenk-type equilibration to insoluble CaH₂ and unreactive [(^DiP^pBDI)₂Ca].^[17] Monitoring at room temperature by ¹H NMR spectroscopy, however, provided evidence for similar H–D exchange. After three weeks, albeit accompanied by redistribution to ca. 20% [(^DiP^pBDI)₂Ca], the initial 1:1 ratio of intensities of the ^DiP^pBDI g-methine signal and Ca–H signals of 2 at δ 4.83 and δ 4.27 ppm, respectively, changed to approximately 2:1 (Figure S16). During this time period, the singlet hydride signal was transformed into an apparent unresolved 1:2:1 triplet, an observation that we attribute to sequential deuterium ($I = 1$) incorporation and the formation of the previously identified dicalcium hydride-deuteride, 2-d₁.^[5] Although mechanistic and kinetic studies of this process were precluded by the aforementioned solution lability, an assessment of a benzene solution of 2 by EPR spectroscopy provided no evidence of

radical formation, even at more elevated temperatures. DFT calculations were, therefore, carried out to provide insight into the mechanism of the H–D exchange reaction of benzene. A reaction enthalpy profile (Figure 1) was determined at room temperature using the B3PW91 functional that has proven its ability to describe group 2 reactivity.^[5,6] Consistent with the slow transformation observed, this process requires the assembly of a number of higher energy intermediates. As in previous studies,^[3,5] the reaction is initiated by nucleophilic attack of a hydride of the dimeric complex 2 on benzene. The resultant disruption of the p electron delocalization in the benzene ring ensures that the associated barrier is rather high (35.5 kcalmol⁻¹). The system is able to evolve from this transition state, however, to a dicalcium benzenyl intermediate, C(benzene), that retains a single Ca–m₂–H–Ca linkage. While C(benzene) is also high in energy (+ 20.6 kcalmol⁻¹), it is sufficiently stabilized by an interaction between the remaining p density and the calcium centers to allow a facile 90° rotation of the benzenyl ligand to yield a further intermediate, D(benzene). Although this process incurs the loss of the benzenyl p–interaction, its replacement by a C@H interaction with one Ca center facilitates delivery of a benzene hydrogen atom back to calcium. Although the barrier associated with this latter process, TS–DE(benzene), is only 7.8 kcalmol⁻¹ and the overall H/D exchange is effectively athermic, the high energies associated with C(benzene) and D(benzene) dictate that such processes are unlikely to exert any significant impact during reactions of 2 with more reactive or readily reducible PAH substrates.

A reaction performed at room temperature between compound 2 and naphthalene in C₆D₆ provided the slow development of a deep blue solution over the course of 60 days. Appraisal by ¹H NMR spectroscopy throughout this time period indicated consumption of ca. 50% of compound 2 and the production of a new compound (9). This latter species comprised two differentiated ^DiP^pBDI ligand environments, which were most clearly characterized by a pair of g-methine resonances at δ 5.46 and 5.10 ppm and which emerged in a strict 1:2 ratio of intensities throughout the course of the reaction. Compound 9 also displayed a characteristic (1H) singlet signal at δ 9.05 ppm, which was subsequently assigned as a [Ca–m₂–H–Ca] bridging hydride environment (see below). While further experiments demonstrated that the reaction time under these conditions could be reduced to one week through the introduction of a ten-fold excess of naphthalene,

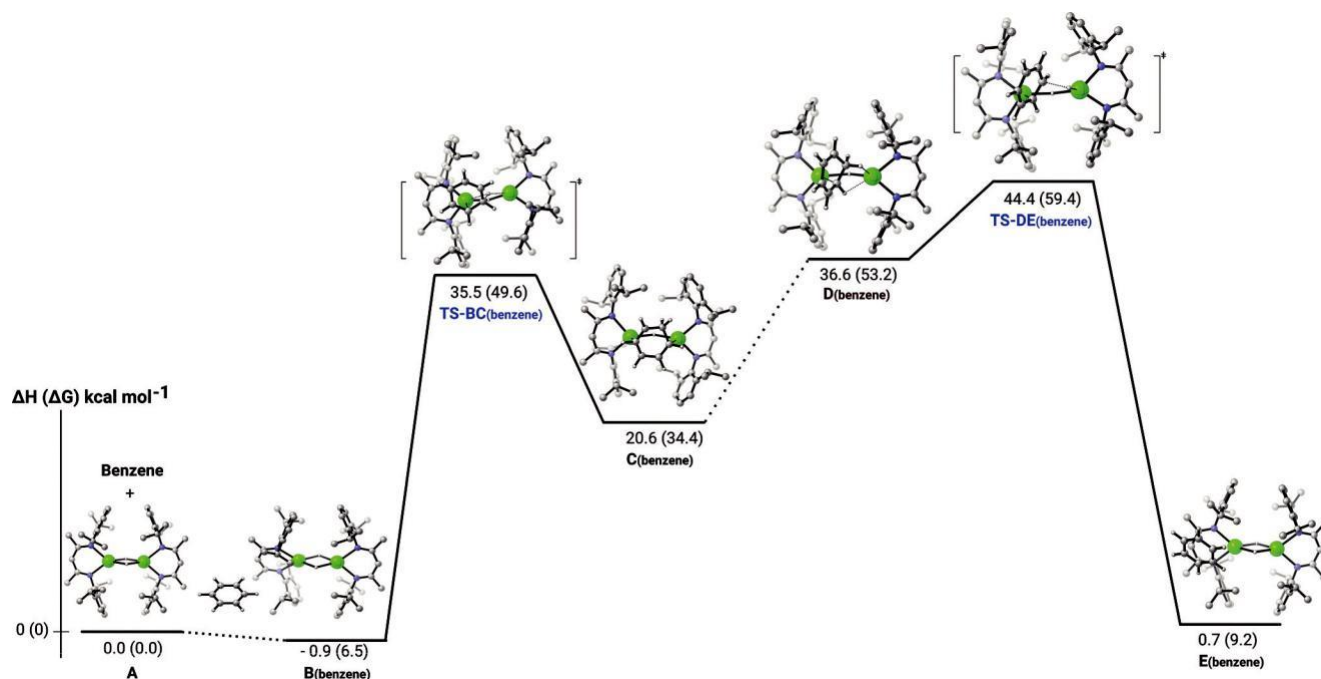


Figure 1. Computed enthalpy profile at room temperature for the H/D exchange reaction catalyzed by compound 2. Gibbs Free energies are given in parenthesis.

the greatest improvements were obtained by performance of the reaction in the absence of any solvent. Simply heating compound 2 and ten equivalents of naphthalene for 1 hour at 808C, after removal of excess naphthalene by sublimation, yielded a blue powder, which was observed to comprise predominantly of compound 9 by ^1H NMR spectroscopy. Crystallization of compound 9 from a saturated toluene/ hexane solution provided blue single crystals suitable for X-ray diffraction analysis, the results of which are shown in Figure 2.

The solid-state structure of compound 9 contains three unique D^{iPPBDI} -ligated calcium environments. Ca1 interacts via an h^6 -interaction with one C_6 ring of a planar naphthalenide dianion. The resultant $\text{Ca1}\cdots\text{C}$ contacts [range 2.681(2) @ 2.887(2) &] are intermediate between the very short distances observed in Westerhausen's unique Ca^{I} species, $[(\text{THF})_3\text{Ca}(\text{m-C}_6\text{H}_3\text{-1,3,5-Ph}_3)\text{Ca}(\text{THF})_3]$ [2.586(3), 2.598(3) &],^[18] and those of the recently reported charge-separated cation in $[(\text{D}^{\text{iPPBDI}})\text{Ca}(\text{C}_6\text{H}_6)]^+ [\text{Al}\{\text{OC}(\text{CF}_3)_3\}_4]^\ominus$ [2.932(5), 2.935(5) &], wherein a molecule of benzene is bound in a h^6 fashion to the calcium center but without any necessary level of reduction.^[19] The remaining two $[(\text{D}^{\text{iPPBDI}})\text{Ca}]$ units bind to the obverse face of the arene dianion through what are best described as h^4 -interactions with $\text{Ca}\text{@C}$ distances in the range 2.770(2)–2.981(2) & to each of the two fused C_6 carbocycles, while overall charge balance is maintained by a hydride anion which bridges Ca2 and Ca3.

Reflecting their more accessible reduction potentials, reactions of the tri- and tetracyclic PAHs, anthracene and tetracene, with compound 2 proceeded more readily in toluene to provide compounds 10 and 11, respectively. Reminiscent of the data provided by 9, the ^1H NMR spectrum of compound 10 was consistent with a structure comprising

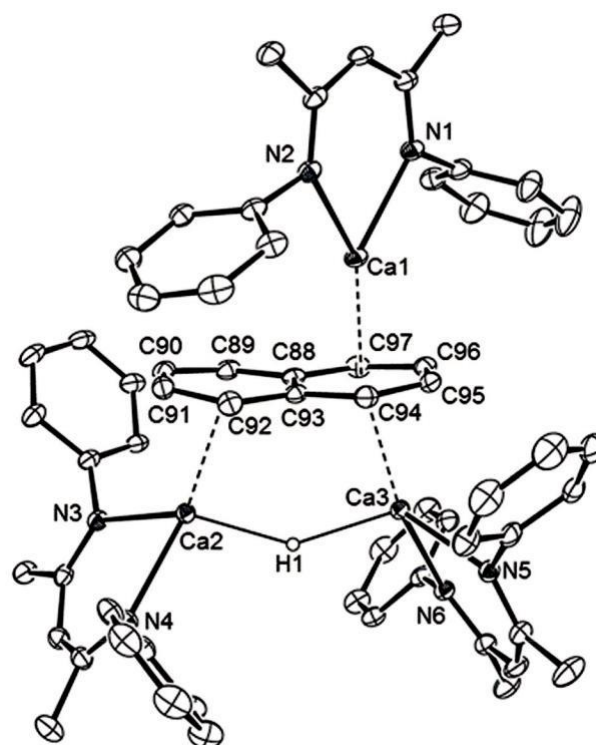


Figure 2. ORTEP representation (30% probability ellipsoids) of compound 9. Hydrogen atoms, except for H1, and iso-propyl groups have been removed for clarity. Selected bond lengths [Å] and angles [°]: Ca1–N1 2.3327(18), Ca1–N2 2.3735(16), Ca1–C88 2.8526(19), Ca1–C93 2.769(2), Ca1–C94 2.681(2), Ca1–C95 2.701(2), Ca1–C96 2.792(2), Ca1–C97 2.887(2), Ca2–N3 2.3859(16), Ca2–N4 2.4057(18), Ca2–C89 2.962(2), Ca2–C90 2.734(2), Ca2–C91 2.718(2), Ca2–C92 2.937(2), Ca3–N5 2.3744(17), Ca3–N6 2.4176(16), Ca3–C94 2.981(2), Ca3–C95 2.770(2), Ca3–C96 2.770(2), Ca3–C97 2.947(2); N1–Ca1–N2 75.09(6), N3–Ca2–N4 79.33(6), N5–Ca3–N6 77.54(6).

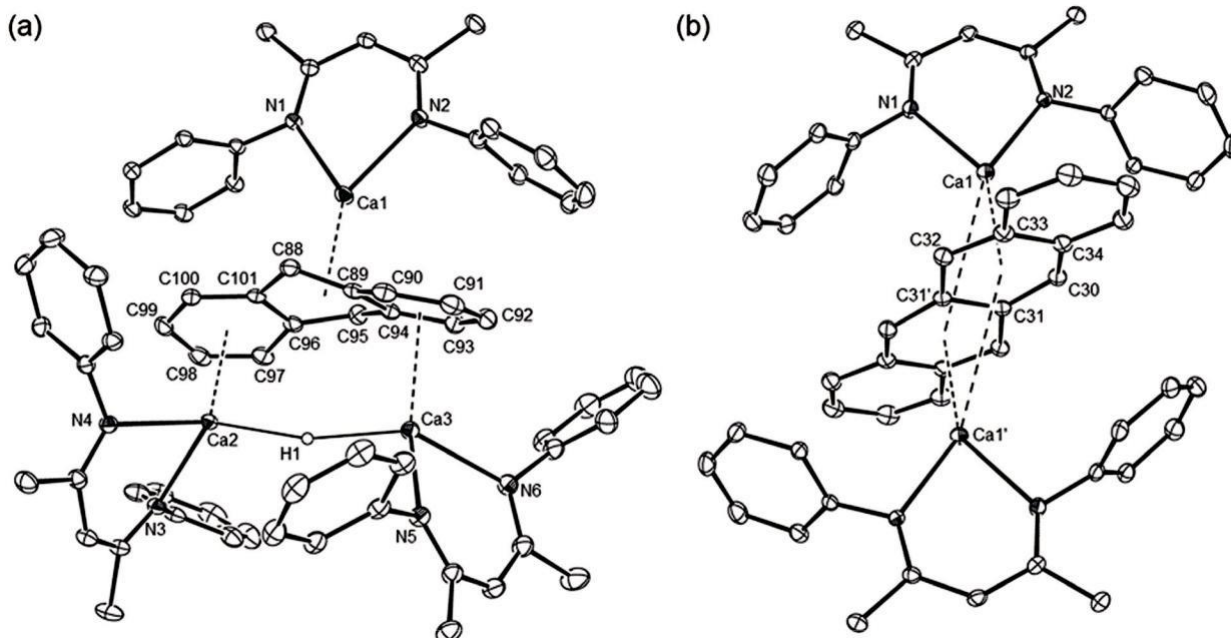


Figure 3. ORTEP representations (30% probability ellipsoids) of a) compound 10 and b) compound 11. Hydrogen atoms, except H1 of compound 10, iso-propyl groups and occluded solvent are removed for clarity. Selected bond lengths [Å] and angles [°]: (10) Ca1–N1 2.3204(17), Ca1–N2 2.3411(17), Ca1–C88 2.651(2), Ca1–C89 2.923(2), Ca1–C94 2.838(2), Ca1–C95 2.624(2), Ca1–C96 3.019(2), Ca2–N3 2.3492(17), Ca2–N4 2.4179(18), Ca2–C96 3.071(2), Ca2–C97 2.981(2), Ca2–C98 2.858(2), Ca2–C99 2.748(2), Ca2–C100 2.712(2), Ca2–C101 2.868(2), Ca3–N5 2.3902(18), Ca3–N6 2.4405(19), Ca3–C89 3.138(2), Ca3–C90 2.995(2), Ca3–C91 2.875(2), Ca3–C92 2.804(2), Ca3–C93 2.801(2), Ca3–C94 2.964(2); N1–Ca1–N2 78.05(6), N3–Ca2–N4 77.51(6), N5–Ca3–N6 78.73(6); (11) Ca1–N1 2.3290(12), Ca1–N2 2.3412(12), Ca1–C30 2.7127(15), Ca1–C31 2.8973(15), Ca1–C32 2.7097(14), Ca1–C33 2.7711(14), Ca1–C34 2.7660(15); N1–Ca1–N2 76.92(4). Symmetry operations to generate equivalent atoms 1@x, 1@y, 1@z.

a 1:2 ratio of two dissimilar $\text{D}^{\text{ipp}}\text{BDI}$ environments along with a single residual Ca–H proton environment, which manifested as a (1H) singlet signal resonating at δ 5.12 ppm. In contrast, the NMR data arising from compound 11 were consistent with the presence of two identical $\{(\text{D}^{\text{ipp}}\text{BDI})\text{Ca}\}$ units, symmetrically disposed about a reduced tetracene dianion. The veracity of these deductions was confirmed by the isolation of purple (10) and blue (11) single crystals of both compounds suitable for X-ray diffraction analysis from toluene and benzene, respectively (Figure 3).

The gross features of compound 10 (Figure 3 a), a trimetallic species featuring formally monocationic $[(\text{D}^{\text{ipp}}\text{BDI})\text{Ca}]^+$ and $[(\text{D}^{\text{ipp}}\text{BDI})\text{Ca}-m-\text{H}-\text{Ca}(\text{D}^{\text{ipp}}\text{BDI})]^+$ units residing on opposite faces of the $[\text{C}_{14}\text{H}_{10}]^{2-}$ dianion, are reminiscent of the structure of 9. In the case of 10, however, the Ca1-containing monometallic moiety interacts with the central C_6 unit whereas both of the hydrido-bridged calcium centers are bound with an approximate h^6 disposition to each of the peripheral anthracenyl rings. In common with previously reported alkali metal derivatives of the $[\text{C}_{14}\text{H}_{10}]^{2-}$ dianion,^[20] the formally antiaromatic nature of the reduced PAH is clearly apparent from a pronounced “hinging” of the tricyclic structure at the [C88–C89–C94–C95–C96–C101] ring, such that the mean planes defined by the peripheral C_6 -rings intersect to subtend a dihedral angle of 26.58°.

Compound 11 (Figure 3 b) presents a contrasting and simpler centrosymmetric structure, whereby two identical $[(\text{D}^{\text{ipp}}\text{BDI})\text{Ca}]$ units interact with the opposing faces of the

interior (C30–C34- and C30'–C34'-containing) C_6 -rings of the tetracyclic $[\text{C}_{18}\text{H}_{12}]^{2-}$ dianion.

The formation of compounds 9–11, particularly the generation of the naphthalenide dianion in 9, indicates a reducing potential for compound 2 that is at least equivalent to or surpasses that of elemental calcium metal and molecular Mg^{I} compounds such as 5 and 6. Evans and co-workers have previously made similar observations through comparison of the reactivity of Cp^*_2Sm (12) and Cp^*_2SmH (13), which contain formally reducing Sm^{2+} and fully oxidised Sm^{3+} centers, respectively ($E^0 \text{Sm}^{3+}/\text{Sm}^{2+}$ @2.304 V).^[21,22] Although neither samarium compound was reactive toward naphthalene, compound 12 effects two electron reduction of both anthracene and tetracene. Treatment of anthracene with compound 13 was also observed, albeit with less discrimination, to provide the identical reduction product, $[(\text{Cp}^*_2\text{Sm})_2(m-h^3 :h^3-\text{C}_{14}\text{H}_{10})]$, along with the formation of H_2 .^[21] Although no mechanistic discussion was included in these earlier reports, examination of in situ ^1H NMR spectra recorded during reactions to provide compounds 9–11 confirmed the similar production of dihydrogen, observed as a resonance at δ 4.46 ppm, prompting a more detailed assessment of the mode of reaction of compound 2 with PAHs.

Reactions of 2 with naphthalene, anthracene and tetracene performed at 350 K within the cavity of a CW EPR spectrometer provided no evidence for the production of short lived hydrogen radicals. In each case, however, signals

arising from the PAH radical anions, $[C_{10}H_8]^{C@}$, $[C_{14}H_{10}]^{C@}$ and $[C_{18}H_{12}]^{C@}$, were readily observed and confirmed by comparison to simulated spectra of the fully delocalized products of single electron reduction (Figure S17). While these data indicate that the formation of the fully reduced PAH dianions is likely to occur via sequential single electron reduction, they provide no compelling evidence for the mode of electron transfer or the production of the dihydrogen by-product. To further assess the nature of these processes, therefore, DFT calculations were performed on the complete system resulting from the reaction between compound 2 and tetracene. The formation of the resultant bimetallic compound (11) was reasoned to provide the necessary insight whilst limiting the computational expense that would have been incurred by a similar study of the formation of either trimetallic derivative, 9 or 10. Possible reaction profiles yielding the formation of 11 were computed at the DFT level (B3PW91), varying the methine C@H unit involved in the reaction on the arene molecule (denoted as positions f, g and h in Figure 4). As described for the H/D exchange of benzene, reaction is initiated by the nucleophilic addition of a hydride of compound 2 to the tetracene molecule (TS-BC). The activation barrier (ca. 28–30 kcalmol⁻¹) associated with this attack varies with the position of hydride addition and may be compared to the analogous process computed for COT (21.8 kcalmol⁻¹).^[7] Following the intrinsic reaction coordinate in all cases leads to the formation of dicalcium tetracene intermediates (Cf/Ch/Cg) that retain a Ca-m₂-H-Ca linkage similar to that identified during the reaction with benzene. While there is little to discriminate the kinetic facility of the nucleophilic attack, the formation of intermediates Cf-h is endothermic due to the disruption of the tetracene p system and their relative stabilities depend on the position of hydride addition (Cf, 16.1; Cg 13.7; Ch 6.2 kcalmol⁻¹). Irrespective of the consequent low productivity of the hydride addition step, however, Cf-h can evolve further intermediates, Df-h, that comprise the experimentally observed tetracene radical anion upon loss of hydrogen radical. In contrast to the appreciably exothermic formation of Df and Dg from their respective parent species, the transformation of Ch to Dh was computed to be effectively isoenergetic. While production of any of Df,

Dg and Dh enables the formation of 11 through a second cascade of nucleophilic hydride addition and hydrogen radical release (see Figure S18), the comparable energies of Ch and Dh allow the identification of a further kinetically favored pathway to 11. This alternative process (Figure S19) involves direct H₂ formation through hydride addition and intramolecular hydride deprotonation in a similar manner to that computed for the aromatization of COT by 2 (Scheme 1). Although the production of the tetracene radical anion was unambiguously observed during the formation of 11, the simultaneous operation of both one- and two-electron based mechanisms should not be discounted. We are comfortable to suggest, therefore, that the more complex trimetallic structures of compounds 9 and 10 may be a reflection of competing kinetic pathways, both inter- and intramolecular, leading to the two-electron reduction process.

In conclusion, the ability of compound 2 to effect the two electron reduction of naphthalene implies that its reducing potency is at least comparable to now well established dinuclear Mg^I reagents. The emerging reactivity of heavier group 2 hydrides and related reagents, particularly for the nucleophilic activation of electron rich arenes, however, indicates that they will continue to provide a complementary source of unprecedented reactivity. We and others are continuing to investigate these possibilities.

CCDC 1962140, 1962141 and 1962142 contain the supplementary crystallographic data for this paper. These data can be obtained free of charge from The Cambridge Crystallographic Data Centre.

Acknowledgements

We thank the EPSRC (UK) for the support of a DTP studentship (A.S.S.W.).

Conflict of interest

The authors declare no conflict of interest.

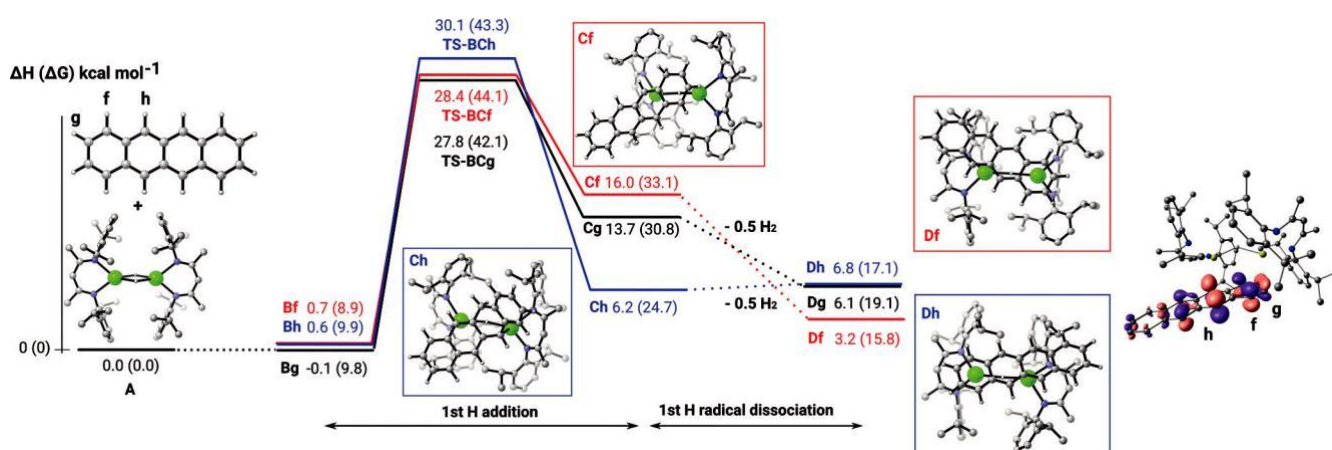


Figure 4. Computed enthalpy profile at room temperature for the reaction of 2 with tetracene. The Gibbs Free energies are given in parenthesis. The calculated SOMO of species D is shown on the far right hand side.

Keywords: calcium · DFT calculations · hydrides · main group chemistry · reduction

How to cite: *Angew. Chem. Int. Ed.* 2020, 59, 1232 – 1237
Angew. Chem. 2020, 132, 1248 – 1253

- [1] a) S. Harder, *Chem. Commun.* 2012, 48, 11165 – 11177; b) D. Mukherjee, J. Okuda, *Angew. Chem. Int. Ed.* 2018, 57, 1458 – 1473; *Angew. Chem.* 2018, 130, 1472 – 1488; D. Mukherjee, D. Schuhknecht, J. Okuda, *Angew. Chem. Int. Ed.* 2018, 57, 9590 – 9602; *Angew. Chem.* 2018, 130, 9736 – 9749; c) J. Spielmann, S. Harder, *Chem. Eur. J.* 2007, 13, 8928 – 8938; d) A. Causero, G. Ballmann, J. Pahl, C. Farber, J. Intemann, S. Harder, *Dalton Trans.* 2017, 46, 1822 – 1831; e) B. Maitland, M. Wiesinger, J. Langer, G. Ballmann, J. Pahl, H. Elsen, C. Farber, S. Harder, *Angew. Chem. Int. Ed.* 2017, 56, 11880 – 11884; *Angew. Chem.* 2017, 129, 12042 – 12046; f) M. Wiesinger, B. Maitland, C. Farber, G. Ballmann, C. Fischer, H. Elsen, S. Harder, *Angew. Chem. Int. Ed.* 2017, 56, 16654 – 16659; *Angew. Chem.* 2017, 129, 16881 – 16886; g) P. Jochmann, J. P. Davin, T. P. Spaniol, L. Maron, J. Okuda, *Angew. Chem. Int. Ed.* 2012, 51, 4452 – 4455; *Angew. Chem.* 2012, 124, 4528 – 4531; h) V. Leich, T. P. Spaniol, J. Okuda, *Inorg. Chem.* 2015, 54, 4927 – 4933; i) C. N. de Bruin-Dickason, T. Sutcliffe, C. A. Lamsfus, G. B. Deacon, L. Maron, C. Jones, *Chem. Commun.* 2018, 54, 786 – 789; j) X. H. Shi, C. P. Hou, C. L. Zhou, Y. Y. Song, J. H. Cheng, *Angew. Chem. Int. Ed.* 2017, 56, 16650 – 16653; *Angew. Chem.* 2017, 129, 16877 – 16880.
- [2] S. Harder, J. Brettar, *Angew. Chem. Int. Ed.* 2006, 45, 3474 – 3478; *Angew. Chem.* 2006, 118, 3554 – 3558.
- [3] B. Rçsch, T. X. Gentner, H. Elsen, J. Langer, M. Wiesinger, S. Harder, *Angew. Chem. Int. Ed.* 2019, 58, 5396 – 5401; *Angew. Chem.* 2019, 131, 5450 – 5455.
- [4] A. S. S. Wilson, M. S. Hill, M. F. Mahon, *Organometallics* 2019, 38, 351 – 360.
- [5] A. S. S. Wilson, M. S. Hill, M. F. Mahon, C. Dinoi, L. Maron, *Science* 2017, 358, 1168 – 1171.
- [6] A. S. S. Wilson, C. Dinoi, M. S. Hill, M. F. Mahon, L. Maron, *Angew. Chem. Int. Ed.* 2018, 57, 15500 – 15504; *Angew. Chem.* 2018, 130, 15726 – 15730.
- [7] M. S. Hill, M. F. Mahon, A. S. S. Wilson, C. Dinoi, L. Maron, E. Richards, *Chem. Commun.* 2019, 55, 5732 – 5735.
- [8] a) F. J. Smentowski, G. R. Stevenson, *J. Am. Chem. Soc.* 1967, 89, 5120 – 5121; b) F. J. Smentowski, G. R. Stevensn, *J. Am. Chem. Soc.* 1969, 91, 7401 – 7402; c) F. J. Smentowski, G. R. Stevenson, *J. Phys. Chem.* 1969, 73, 340 – 341.
- [9] a) A. Stasch, C. Jones, *Dalton Trans.* 2011, 40, 5659 – 5672; b) C. Jones, *Nat. Rev. Chem.* 2017, 1, 0059.
- [10] a) A. V. Zabula, M. A. Petrukhina, *Adv. Organomet. Chem.* 2013, 61, 375 – 462; b) J. E. Ellis, *Dalton Trans.* 2019, 48, 9538 – 9563.
- [11] a) B. Bogdanovic, *Acc. Chem. Res.* 1988, 21, 261 – 267; b) E. Bartmann, B. Bogdanovic, N. Janke, S. J. Liao, K. Schlichte, B. Spliethoff, J. Treber, U. Westeppe, U. Wilczok, *Chem. Ber. Rec.* 1990, 123, 1517 – 1528; c) H. Bonnemann, B. Bogdanovic, R. Brinkmann, N. Egeler, R. Benn, I. Topalovic, K. Seevogel, *Main Group Met. Chem.* 1990, 13, 6; d) A. Uresk, N. J. O Neil, Z. Zhou, Z. Wei, M. A. Petrukhina, *J. Organomet. Chem.* 2019, 897, 57 – 63.
- [12] N. G. Connelly, W. E. Geiger, *Chem. Rev.* 1996, 96, 877 – 910.
- [13] a) J. J. Brooks, W. Rhine, G. D. Stucky, *J. Am. Chem. Soc.* 1972, 94, 7346 – 7347; b) C. Melero, A. Guijarro, M. Yus, *Dalton Trans.* 2009, 1286 – 1289.
- [14] S. Kriek, L. Yu, M. Reiher, M. Westerhausen, *Eur. J. Inorg. Chem.* 2010, 197 – 216.
- [15] S. R. Lawrence, C. A. Ohlin, D. B. Cordes, A. M. Z. Slawin, A. Stasch, *Chem. Sci.* 2019, <https://doi.org/10.1039/C9DT03976G>.
- [16] a) M. E. Thompson, S. M. Baxter, A. R. Bulls, B. J. Burger, M. C. Nolan, B. D. Santarsiero, W. P. Schaefer, J. E. Bercaw, *J. Am. Chem. Soc.* 1987, 109, 203 – 219; b) M. Booiij, B. J. Deelman, R. Duchateau, D. S. Postma, A. Meetsma, J. H. Teuben, *Organo-metallics* 1993, 12, 3531 – 3540; c) G. Jeske, H. Lauke, H. Mauermann, H. Schumann, T. J. Marks, *J. Am. Chem. Soc.* 1985, 107, 8111 – 8118.
- [17] a) S. Harder, *Organometallics* 2002, 21, 3782 – 3787; b) A. G. Avent, M. R. Crimmin, M. S. Hill, P. B. Hitchcock, *Dalton Trans.* 2005, 278 – 284.
- [18] S. Kriek, H. Gçrls, L. Yu, M. Reiher, M. Westerhausen, *J. Am. Chem. Soc.* 2009, 131, 2977 – 2985.
- [19] L. Garcia, M. D. Anker, M. F. Mahon, L. Maron, M. S. Hill, *Dalton Trans.* 2018, 47, 12684 – 12693.
- [20] a) W. E. Rhine, J. Davis, G. Stucky, *J. Am. Chem. Soc.* 1975, 97, 2079 – 2085; b) W. E. Rhine, J. H. Davis, G. Stucky, *J. Organomet. Chem.* 1977, 134, 139 – 149; c) H. Bock, K. Gharagozloo-Hubmann, M. Sievert, T. Prisner, Z. Havlas, *Nature* 2000, 404, 267 – 269.
- [21] W. J. Evans, S. L. Gonzales, J. W. Ziller, *J. Am. Chem. Soc.* 1994, 116, 2600 – 2608.
- [22] W. J. Evans, B. M. Schmiede, S. E. Lorenz, K. A. Miller, T. M. Champagne, J. W. Ziller, A. G. DiPasquale, A. L. Rheingold, *J. Am. Chem. Soc.* 2008, 130, 8555 – 8563.